DEPENDENCE OF ION FLOW THROUGH CHANNELS ON THE DENSITY OF FIXED CHARGES AT THE CHANNEL OPENING

Voltage Control of Inverse Titration Curves

BERND LINDEMANN
Second Department of Physiology, Universität des Saarlandes, 6650 Homburg/Saar, Federal Republic of Germany

ABSTRACT Model calculations were done to investigate the effect of titratable fixed charges at channel openings on ion flow through open channels. The current titration curves (channel current vs. bulk pH) can assume the shape expected from the change of the ionic surface concentration with pH (c-control), or be inverted, i.e., follow the change of the electrical field within the membrane (V-control). The relationships were explored *pars pro toto* for Goldman-Hodgkin-Katz channels, two-barrier one-site channels and six-barrier five-site channels. With net current flowing in the direction of the concentration gradient and from the titrated fixed charge layer into the channel, c-control is the sign of low channel occupancy (entrance-step limitation) and V-control the sign of high channel occupancy (exit-step limitation). At intermediate occupancy, the current titration curve can be nearly invariant to pH.

INTRODUCTION

Titration of membrane fixed charges is a common procedure in the investigation of transport properties of biological membranes. The literature distinguishes specific fixed charges within a channel and unspecific charges outside the channel, at the membrane surface (e.g., Drouin and Neumcke, 1974). Occupation of a specific negative charge by a proton results in blockage of cation flow through the channel. Titration of unspecific charges with protons as well as altered charge-screening in the diffuse double layer results in a change of the electrical field within the membrane. In consequence, voltage-dependent gating will then occur at a different overall membrane voltage (e.g., Mozhayeva and Naumov, 1972).

In addition to changing the electrical field within the membrane, the titration of unspecific charges will also change the concentration of ions at the membrane surface. The effects of concentration and field affect ion flow oppositely, but do not necessarily cancel. In fact, one may presume that the concentration effect dominates, because only a fraction of the electrical field will operate on any one rate-limiting diffusional step within the membrane.

In this paper, the effect of surface fixed charges on channel currents is studied by means of several simple channel models combined with the theory of diffuse double-layers. While more realistic models for channel and charge layer could have been used, their added algebraic difficulties merely distract from the principal point to be made. The question emphasized is whether a cationic current passing the open, ungated channel will always decrease, or change at all, when negative fixed charges are removed from the membrane surface close to the channel opening, and which properties of the channel itself will be reflected in the current titration curve. To my knowledge, no one has yet dealt with these questions in a systematic way.

RESULTS

Homogeneous Channels

The permeability of channels with a very large number of diffusional energy barriers of equal height can be described by a single parameter, the concentration- and voltage-independent permeability constant P (Eyring et al., 1949; Woodbury et al., 1970). The current-voltage curve of such channels, which obeys the GHK- or "constant-field" equation (Goldman, 1943; Hodgkin and Katz, 1949) has a curvature that is solely due to the asymmetry of ion concentrations at the two openings of the channel. Inasmuch as flow through such channels constitutes a particularly simple case of nonsaturating electrodiffusional transport, we shall use the homogeneous channels as the first model for studying the effect of surface fixed charges. The computational details are so well known that a brief description of the assumptions used in the calculation will suffice. More details are found in the papers cited.

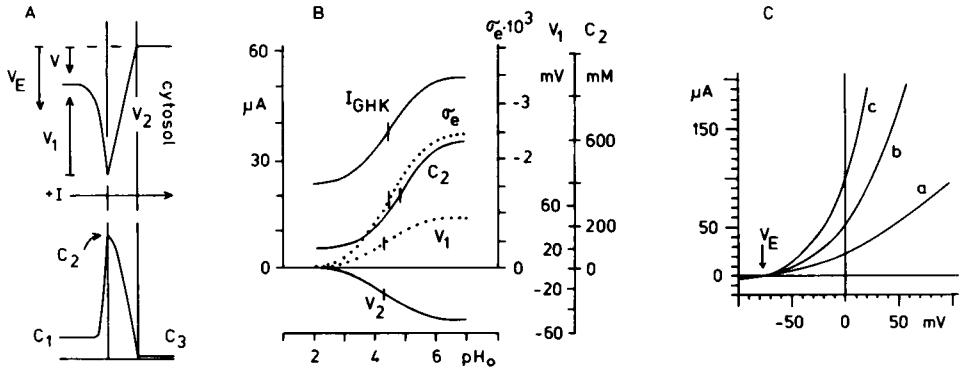

FIGURE 1 *A*, schematic voltage profile across membrane and diffuse double layer at the outer membrane surface. The two vertical lines delimit the length of membrane-spanning channels. Scale of abscissa is arbitrary. The outer membrane surface has negative fixed charges; the fixed charge density at the cytosol opening of the channels is set to zero (throughout this paper). Voltage reference is the potential of the cytosol (this convention is suitable for the analysis of current flow through apical epithelial membranes). The case of a negative overall clamp voltage, V, is shown. V_1 assumes a positive and V_2 a negative value, such that $V = V_1 + V_2$. V_E is the equilibrium potential for a given pair of c_1 and c_3. With $V > V_E$, positive net current will flow as indicated by the horizontal arrow. The lower part of *A* shows schematically the activity profile of a cationic species passing a GHK-channel. *B*, *c*-controlled current titration curve (upper solid line) of homogenous channels (GHK-channels) at an overall clamp voltage of $V = 0$ mV. Shown below are σ_e, V_1, V_2, and c_2 as a function of bulk pH. Parameters are as follows: $\sigma_i = -0.0025$ charges Å^{-2} ($0.4 \cdot 10^{-5}$ C cm^{-2}; with the charges arranged in a square lattice, their shortest distance would be 20 Å when all are dissociated.) p$K_H = 4$, $c_1 = 90$, $c_3 = 4$ mM activity. Ca activity of outer solution, 0.7 mM; ionic strength, 92.1 mM; Debye length, 10.1 Å; permeability, $0.25 \cdot 10^{-5}$ cm s^{-1}; temperature, 20°C. *C*, current-voltage curves of GHK-channel at pH$_o$ = 7. The permeability was $0.25 \cdot 10^{-5}$ cm s^{-1} for all three curves. σ_i was varied such that for curves *a*, *b*, and *c*, σ_i was 0, -0.0025, and -0.01 Å^{-2}. This resulted in V_1 values of 0, 47.2, and 100 mV. Other parameters as in *B*.

The GHK-equation (constant-field current-voltage relationship) for a channel permeable to one ionic species may be written

$$I = FP\frac{V_2/(RT/F)}{1-\xi}(c_2 - c_3\xi), \qquad (1)$$

in which V_2 stands for the voltage across the channel, the cell interior being the reference point,[1] c_2 and c_3 are the activities of the permeant species at the channel openings, P the permeability, and I the current through the channel. R, T, and F have their usual meaning and ξ is an abbreviation defined as

$$\xi = \exp[-V_2/(RT/F)].$$

V_2 and c_2 will change with the fixed charge density at the outward-facing membrane surface.

Suppose that at the outer membrane surface around the channel opening there is a layer of acidic groups of uniform pK_H and of uniform site density corresponding to a maximal charge density of σ_i (electronic charges Å^{-2}). The degree of dissociation of these groups and thus the effective negative fixed charge density σ_e is determined by the proton activity $(H)_2$ at the membrane surface,

$$\sigma_e = \sigma_i[1 + (H)_2/K_H]^{-1},$$

K_H being the proton dissociation constant. The binding of other ions is excluded. $(H)_2$ in turn depends on the bulk pH and the surface potential V_1:

$$(H)_2 = (H)_1 \cdot \exp[V_1/(RT/F)]$$

in which $(H)_1$ is the proton activity in the outer solution[2] and V_1 the electrical potential of the outer solution with respect to that of the fixed charge layer (see Fig. 1*A*). For a given σ_e, the resulting V_1 is strongly dependent on the screening effect of ions contained in the diffuse double layer. For a given set of bulk ionic activities, matching values of σ_e and V_1 may be calculated iteratively with the Grahame equation (e.g., McLaughlin et al. 1971). At this point the idealizations contained in the Gouy-Chapman theory enter into the computation. Note, however, that *for our purposes* a mismatch between the true σ_e and V_1 is not important as long as V_1 and c_2 have the right relationship. Subsequently, the surface activity of the permeant species

$$c_2 = c_1 \cdot \exp[V_1/(RT/F)]$$

and the voltage across the channel itself,

$$V_2 = V - V_1,$$

can be calculated for a given overall membrane voltage V, c_1 being the activity in the outer solution. The current is then computed with Eq. 1, assuming that equilibration of bulk concentrations with the double layer is fast enough, so that c_2 will not decrease when I assumes large values (compare Läuger, 1976).

[1]This convention is used in the study of apical epithelial membranes.

[2]More strictly, concentrations rather than activities should be used for the Boltzman distribution.

Fig. 1*B* shows a calculated titration curve of the net current and several variables that are a function of bulk outside pH. With a σ_t of -0.0025 Å^{-2} and a pK_H of 4, σ_e, c_2, and V_1 increase with increasing pH_0; only V_2 decreases. The bulk activities of the permeant ion species were chosen as $c_1 = 90$ mM in the outer solution and $c_2 = 4$ mM at the protoplasmic side of the membrane. Because of the increase in V_1 to 47.4 mV at high pH values, c_2 approaches 594 mM at pH 8. With the outer Ca activity set to 0.7 mM, that at the membrane surface reaches 29 mM at pH 8. The net current, calculated for an overall membrane potential of 0 mV and a permeability of 0.25×10^{-5} cm · s^{-1}, also increases with the pH. Clearly, the increase in c_2 over c_1 affects I more than the counteracting decrease in V_2 does.

A current-titration curve that follows the general shape of the c_2 (pH_0) function will be called concentration-controlled (*c*-controlled). In contrast, a curve that follows the general shape of the V_2 (pH_0) function will be called inverted or *V*-controlled. Usually, a titration curve will be affected by both the concentration and voltage effect, with one of them dominating. In Fig. 1*B*, *c*-control is dominant. That the counteracting effect of the electrical field is, nevertheless, operative, can be seen from the apparent p*K* value (4.4) of the $I(pH_0)$ curve, which is slightly smaller than the apparent p*K* value of the σ_e curve (4.5 at a true pK_H of 4.0). For the parameter values mentioned, the inflection point of the $I(pH_0)$ function increases somewhat with clamp voltage, reaching 4.8 at $V = +66$ mV (not shown). The apparent p*K* values of the other curves are also above p$K_H = 4$ as expected from the *H*-activity ratio between bulk solution and membrane surface. It is noteworthy, however, that the inflection points of these curves are all different.

When V is clamped to the equilibrium potential $V_E = (RT/F) \cdot \ln(c_3/c_1)$ the current is zero at all pH_0 values. In this case the concentration change (c_2) and the voltage change (V_2) caused by the titration have equal and opposite effects. It is noteworthy that with V clamped to values more negative than the equilibrium potential, inverse titration curves result (see Fig. 5*A*). Here the voltage effect on the now dominating negative unidirectional current is larger than the combined concentration and voltage effect on the vanishing positive unidirectional current (*V*-control). Thus inverted titration curves must be expected from GHK-channels if the net cationic current flows towards that membrane surface where the fixed charges are titrated. Similarly, *V*-control dominates when c_1 is made small with respect to c_3 (see below).

The computed titration curves are not as steep as those that would be obtained experimentally, because at low pH, where σ_e approaches small values, the perfect field overlap assumed by the Gouy-Chapman theory is impossible. In consequence, experimental apparent p*K*-values may be somewhat larger than the ones shown in Fig. 1*B*. The ratio of currents observed at the two extremes of the current titration curve (i.e., in the absence and presence of the fixed charges) can be used to estimate V_1. It is easy to show that for a GHK-channel at $V = 0$ mV

$$\frac{I_\sigma}{I_{\sigma=0}} = \frac{FV_1}{RT} \cdot \frac{\exp(FV_1/RT)}{\exp(FV_1/RT) - 1}. \qquad (2a)$$

In Fig. 1*B* this ratio is 2.22, corresponding to a V_1 of 47.1 mV at pH 7. For a single barrier channel the ratio would be

$$\frac{I_\sigma}{I_{\sigma=0}} = \exp(FV_1/2RT), \qquad (2b)$$

which is somewhat larger (2.57) than that of a GHK-channel (compare Neumcke, 1976). The V_1 value thus obtained can then be used to estimate σ_t.

The presence of fixed charges distorts the shape of the GHK-current-voltage curve (Frankenhaeuser, 1960). As the equilibrium potential cannot be affected whereas the currents increase with σ_e, the curvature of the current-voltage relationship increases with σ_e, as shown in Fig. 1*C*. (The resulting curve can be fitted with the GHK-equation when, in addition to P and c_3, V_1 is introduced as a third parameter which then permits us to calculate c_2 and V_2 needed for the fit.) In general, negative fixed charges at the membrane side where the higher concentration of the permeant ion species is found will increase the curvature, whereas fixed charges at the side of lower concentration will decrease the curvature. Therefore, negative fixed charges at the outer membrane surface will make the instantaneous GHK-*IV*-curve for ions distributed like Na more curved while the *IV*-curve for ions distributed like *K* will be less curved.

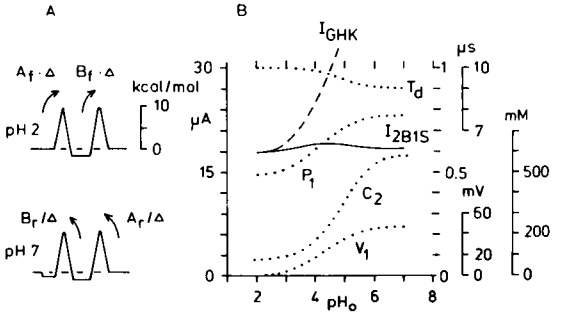

FIGURE 2 *A*, schematic barrier profiles for symmetrical 2B1S-channels in kcal mol^{-1} at a pH_0 of 2 and 7. Abscissa, distance from membrane surface (arbitrary). The diffusional steps corresponding to the forward (f) and reverse (r) entrance (*A*) and exit (*B*) rate constants are indicated by arrows. $A_f = A_r = 10^6$ liter · mol^{-1}s^{-1} and $B_f = B_r = 5 \times 10^4$ s^{-1} was used at a temperature of 20°C. At $pH_0 = 7$, V_1 of 47.2 mV is seen to correspond to an energy valley of 1.1 kcal mol^{-1} in depth. Clamp voltage $V = 0$ mV. *B*, current titration curve of a symmetrical 2B1S channel of moderate occupancy P_1. Clamp voltage $V = 0$ mV. Rate constants are as in panel *A*. Area density of channels, $N = 5 \times 10^9$ cm^{-2} (8.2 fmol of channels/cm^2; mean distance, 1,400 Å). Other parameters are as in Fig. 1*B*. The corresponding titration curve of GHK-channels (of $P = 0.21 \times 10^{-5}$ cm · s^{-1}) is indicated by the dashed line (– – –).

Channel with Two Barriers

To implement saturation behavior, the simplest model is probably a channel with two barriers and one central site that can accommodate not more than one ion (2B1S-channel). The abbreviations for diffusional rate constants used below are given in Fig. 2 *A*. Transport through a 2B1S-channel is characterized by three rate constants, the fourth is given by the condition of microscopic reversibility:

$$A_f \cdot B_f = A_r \cdot B_r.$$

For equal spacing of barrier peaks and energy valleys, a constant electrical field along the channel, and a transmission factor of one, the voltage dependence of the rates will be accounted for by the factor

$$\Delta = \exp[V_2/(4 \cdot RT/F)].$$

With

$$S = c_2A_f\Delta + B_r/\Delta + B_f\Delta + c_3A_r/\Delta$$

being the sum of all rates taken individually (disregarding occupany), the steady-state occupational probabilities of the central site may be written as the sum of rates leading to a state divided by S.[3] Thus, the probabilities for the empty and the occupied state will be

$$P_0 = (B_f\Delta + B_r/\Delta)/S$$

$$P_1 = 1 - P_0 = (c_2A_f\Delta + c_3A_r/\Delta)/S.$$

The mean lifetime of the occupied state (the dwelltime) is $T_d = (B_f\Delta + B_r/\Delta)^{-1}$. The actual net flow across the left barrier will be

$$J_1 = (1/N_L) \cdot (c_2 \cdot A_f \cdot \Delta \cdot P_0 - B_r \cdot \Delta^{-1} \cdot P_1),$$

in which N_L is Avogadro's number. More generally, flow rates across the two barriers may be computed from

$$\begin{pmatrix} J_1 \\ J_2 \end{pmatrix} = \frac{1}{N_L}\begin{pmatrix} c_2A_f\Delta & -B_r/\Delta \\ -c_3A_r/\Delta & B_f \cdot \Delta \end{pmatrix}\begin{pmatrix} P_0 \\ P_1 \end{pmatrix}.$$

In the steady state the two flows are equal and with N denoting the area density of channels we obtain for the current density

$$I = (F \cdot N/N_L) \cdot (c_2A_fB_f\Delta^2 - c_3A_rB_r/\Delta^2)/S \quad (3a)$$

$$= F \cdot \left(\frac{N}{N_L}\right) \cdot \frac{A_fB_f}{S}\Delta^2 \cdot (c_2 - c_3\Delta^{-4}) \quad (3b)$$

as used before (e.g., Lindemann, 1968). Eq. 3 differs from the relationship derived by Parlin and Eyring (1954) in that it is not limited to small concentrations. The overall transport rate is given by the product of forward rates minus the product of reverse rates (disregarding occupancy) divided by the sum of all rates. Since this sum increases with the ionic activities c_2 and c_3, the current through the 2B1S-channel will saturate, for instance, with increasing c_2. The maximal current at very high c_2 and not too large V_2 is

$$I_{max} = (F \cdot N/N_L) \cdot B_f \cdot \Delta \quad (4a)$$

and the half-maximal current will be observed at

$$c_2 = [B_f + B_r/\Delta^2 + c_3(2A_f + A_r)]/A_f. \quad (4b)$$

For $A_f = A_r = 10^6$ liter $\cdot$ mol^{-1} $\cdot$ s^{-1} (symmetrical channel) and $B_f = 5 \times 10^4$ s^{-1} the $I(pH_0)$ curve of Fig. 2 *B* was obtained. Concentrations, fixed charge density, pK_A and overall clamp voltage (0 mV) were those of Fig. 1*B*. It is striking to note that the current varies very little with pH_0, although c_2 increases 6.6-fold (see Fig. 1*B*). There is, however, a slight maximum in the current titration curve which suggests that the invariance of I results from two opposing changes. At low pH_0 the current is limited by the entrance rate, $c_2 \cdot A_f \cdot \Delta \cdot P_0$, such that the increase in c_2 with pH_0 increases I. As a result of this the occupancy P_1 increases as shown in the figure and the current becomes limited by the exit rate, $B_f \cdot \Delta \cdot P_1$. Since the exit rate decreases when V_2 becomes more negative with increasing pH_0, the current decreases again when high pH_0 values are reached. In contrast to P_1, the dwelltime decreases with increasing pH_0: for a given pair of exit-rate constants it will always be maximal when $V_2 = 0$ mV. For comparison, the $I(pH_0)$ function of a GHK-channel is also shown in Fig. 2 *B* (dashed curve). In its computation the permeability was set to

$$P = (N/N_L) \cdot A_f \cdot B_f/S, \quad (5)$$

which is the permeability of a 2B1S channel ensemble at $V_2 = 0$ mV (as can be shown by comparison of Eqs. 1 and 3).

The pH invariance of current through 2B1S-channels, demonstrated for the parameter set of Fig. 2 *B*, is not maintained at all clamp voltages. Therefore, should such an invariance be found experimentally, it has to be confirmed for a wide range of clamp voltages before the conclusion may be drawn that the channel opening is free of titratable fixed charges.

If the titration of surface charges has opposite effects on entrance rate and exit rate, and if the relative importance of the two effects is determined by the occupancy, entirely different current titration curves should be found when the rate constants are chosen for high or low occupancy. This is demonstrated in Fig. 3. For the left diagram, all rate constants were set to 10^6 liter $\cdot$ mol^{-1}s^{-1} or s^{-1}, respectively. In consequence the dwelltime assumes values < 1 μs and the occupancy does not exceed 0.16. The current

[3] In this example, as well as for channels with more barriers, S is generally the determinant of the normalized transition rate matrix of the master equation which describes the kinetic system.

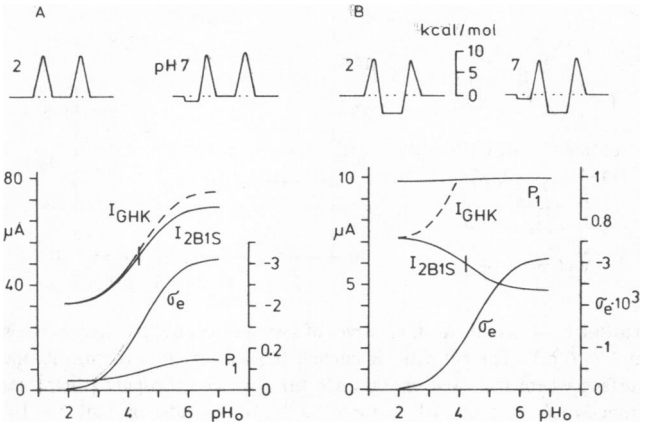

FIGURE 3 Current-titration curves of symmetrical 2B1S channels of low occupancy (*A*) and high occupancy (*B*) at $V = 0$ mV. For both *A* and *B* the net cationic current is directed away from the membrane surface which is titrated. Schematical barrier profiles for $pH_0 = 2$ and $pH_0 = 7$ are indicated above each graph. *A*, *c*-control. Rate constants, $A_f = A_r = 10^6$ liter mol^{-1}s^{-1}; $B_f = B_r = 10^6$ s^{-1}. *B*, *V*-control. $A_f = A_r = 10^7$ liter mol^{-1} s^{-1}; $B_f = B_r = 10^4$ s^{-1}; $N = 5 \times 10^9$ cm^{-2}; other parameters are as in Fig. 1 *B*. The dashed lines indicate GHK-titration curves of $P = 0.38 \times 10^{-5}$ cm s^{-1} (*A*) and 0.083×10^{-5} cm s^{-1} (*B*).

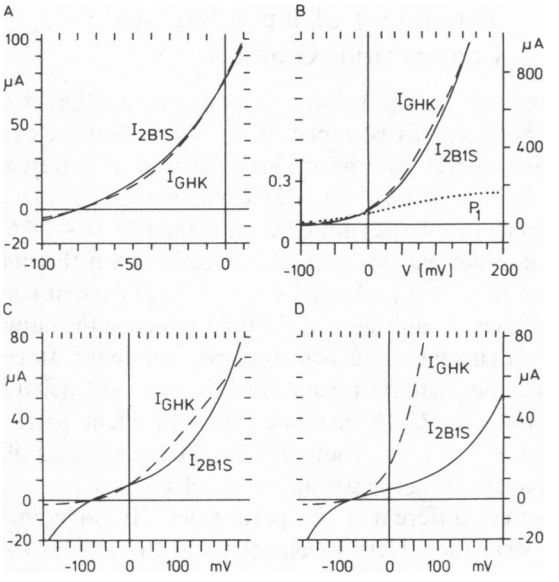

FIGURE 4 Current-voltage curves of symmetrical 2B1S-channels (——) and GHK-channels (– – –) at low occupancy (*A* and *B*) and high occupancy (*C* and *D*). *A* and *B*, $A_f = A_r = 10^6$ liter mol^{-1} s^{-1}; $B_f = B_r = 3 \times 10^6$ s^{-1}; $P = 0.394 \times 10^{-5}$ cm s^{-1}, $pH_0 = 7$. *C* and *D*, $A_f = A_r = 10^7$ liter mol^{-1} s^{-1}; $B_f = B_r = 10^4$ s^{-1}; $P = 0.083 \times 10^{-5}$ cm s^{-1} as in Fig. 3 *B*. pH_0 was 2 for panel *C* and 7 for panel *D*. $N = 5 \times 10^9$ cm^{-2}, other parameters are as in Fig. 1 *B*.

titration curve resembles that of a GHK-channel at the same overall voltage (dashed curve, calculated for $P = 0.383 \times 10^{-5}$ cm · s^{-1} obtained with Eq. 5). The two titration curves can be made to coincide exactly by setting B_f to 3×10^6 s^{-1}. For the right diagram of Fig. 3 an occupancy close to 1 was achieved with the rate constants $A_f = A_r = 10^7$ liter · mol^{-1}s^{-1} and $B_f = 10^4$ s^{-1}. The dwelltime increased to values of 50 μs (at $V_2 = 0$) and the current now decreases with increasing pH_0. Clearly, therefore, an entrance-rate-limited channel, which has a low occupancy, will show a titration curve resembling that of a GHK-channel, because the concentration effect of the fixed charge titration dominates (*c*-control). In contrast, an exit-rate limited channel, which has a high occupancy, will show an inverted titration curve because the voltage effect of the fixed charge titration dominates (*V*-control). At intermediate occupancies the current shows little change with pH_0 (Fig. 2).

If the titration curve matches that of a GHK-channel, it may nevertheless be possible to distinguish the channel types by their current-voltage curves. Examples with low and high fixed charge density are shown in Fig. 4 for low occupancy (*A* and *B*) and high occupancy (*C* and *D*). The outward-going rectification seen in *C* and *D* is a consequence of the high occupancy: B_f/Δ is rate limiting in this branch of the current-voltage curve. *c*-control is, nevertheless, possible in this situation, as discussed below.

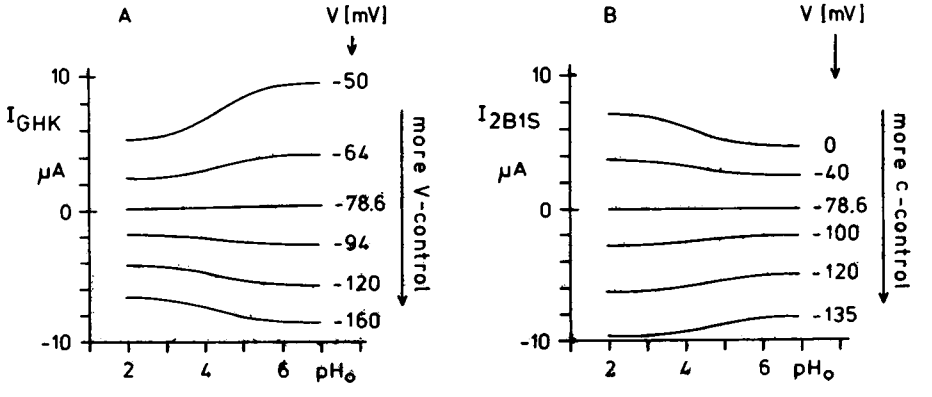

FIGURE 5 Current-titration curves at different overall clamp voltage *V*. *A*, GHK-ensemble current as a function of pH_0. A permeability of 0.272×10^{-5} cm s^{-1} was used for all curves. *V* is as indicated at the curves. Other parameters are as in Fig. 1 *B*. Clamping the outside to more negative voltages causes increasing domination of *V* control, such that the titration curves become inverted. *B*, current through 2B1S-channels of high occupancy as a function of pH_0. The clamp voltage is indicated at the curves, other parameters are as in Fig. 3 *B*. Clamping to outside more negative voltages decreases the occupancy slightly and results in increasing domination of *c* control.

Variation of Clamp Voltage and Concentration Gradient

The overall clamp voltage V will change the channel occupancy. It may be expected, therefore, that the current titration curves assume different shapes at different V. This is first shown for GHK-channels with Fig. 5*A*. Clamping to voltages more negative than $V_E = -78.6$ mV results in net outward current. Together with the magnitude of the inward-directed unidirectional current component c-control vanishes and the field-effect on the outward-directed current component becomes dominant. In consequence, the current titration curve inverts. The behavior is not unique to GHK-channels. An equivalent pattern to that of Fig. 5*A* was computed for 2B1S-channels of low occupancy, using the parameter set of Fig. 3*A*.

Entirely different is the pattern for 2B1S-channels of high occupancy. Here V-control dominates at $V > V_E$ and results in inverted titration curves. However, when clamping to overall voltages more negative than V_E, occupancy decreases somewhat and c-control becomes more dominant: with increasing σ_e at higher pH_0 the forward rate $c_2 \cdot A_f \cdot \Delta \cdot P_0$ across the outer barrier becomes larger, increasing the occupancy even further. As a result the inward-directed current component increases and the net current becomes less negative at high pH_0-values (Fig. 5*B*).

Net outward current can also be achieved by inverting the concentration gradient. At low c_1, c-control becomes difficult and the calculations show (with $V = 0$ mV) inverted current titration curves for GHK-channels as well as √2B1S-channels of low or high occupancy. Therefore, within the framework of these models, inverted titration curves may be expected for K-channels when fixed charges at the outer cell surface are titrated (see Discussion).

The described behavior of the models used can be classified as follows: inverse titration curves result from V-control. At high c_1 and with net current flow directed from the titrated fixed charge layer through the channel, V-control is the consequence of high occupancy (which results from exit-step limited transport). In these cases V-control improves with occupancy. In contrast, when in response to negative clamp voltages net current flows oppositely, V-control improves at lower occupancy. When the concentration gradient is inverted and c_1 is low, the discriminative power becomes poor: then V-control is dominant irrespective of occupancy and current direction.

6B5S-Channel

To obtain titration curves for multiple barrier channels the model of Heckmann et al. (1972) was chosen. It specifies a pore containing an arbitrary number of internal diffusional barriers of uniform height and one limiting barrier of separately adjustable height at each end of the channel. Analytical solutions have been derived for the case of a uniform electrical field and occupation by no more than one ion at a time. These were used here, omitting, however, the Ca block feature discussed by Heckmann et al. The rate constants for four internal barriers were set to $A = 10^8$ s^{-1}. The entrance rate constants were chosen to $A_f = A_r = 10^6$ liter · mol^{-1} s^{-1} (symmetrical channel) and the exit rate constants were varied together to change the occupancy while preserving microscopic reversibility. The fixed charge parameters were those of Fig. 1*B*. Current titration curves for the 6B5S channel are shown in Fig. 6 for four degrees of occupancy. Again low occupancy ($B_f = 10^7$ s^{-1}) results in a c-controlled titration curve resembling that of a GHK-channel (curve *a*). Note, however, that the apparent pK of this curve is far below 4.5, indicating that the voltage effect of the titration is not negligible. With increasing occupancy the voltage effect becomes dominant such that with $B_f = 2 \times 10^5$ s^{-1} an inverted titration curve of rather large apparent pK is obtained (curve *d*). (The dependence of $I(pH_0)$-inflection points on holding voltage and occupancy shows that in the calculation of pK-values of surface charges from current titration curves the nature of the transport channel must be taken into account.) On the whole, the current titration curves of this multi-barrier channel show an occupancy dependence that is similar to those of the 2B1S-channel.

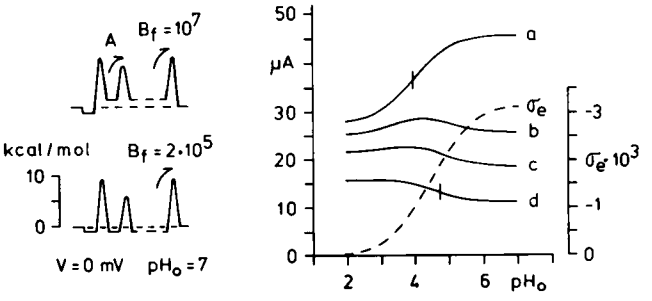

FIGURE 6 Current-titration curves of symmetrical 6B5S-1 ion channels at $V = 0$ mV. The net cationic current flows away from the membrane surface where the fixed charges are titrated. The occupancy increases from *a* to *d*. $A_f = A_r = 10^6$ liter mol^{-1} s^{-1}. Internal rate constant $A = 10^8$ $s^{-1} \cdot B_f = B_r$ was 10^7, 7×10^5, 4×10^5, and 2×10^5 s^{-1} (from *a* to *d*) · $N = 5 \times 10^9$ cm^{-2}, other parameters are as in Fig. 1 *B*. Schematic barrier profiles for curve *a* and *d* ($pH_0 = 7$) are shown on the left. Only one of the four equal internal barriers is indicated.

DISCUSSION

This paper deals with the dependence of channel currents on the membrane's surface fixed charge density.[4] It is found that, depending on the barrier profile of the channel, removal of unspecific fixed charges located near the channel opening may decrease or increase the channel current or leave it unaffected. Therefore, current titration curves permit conclusions about the barrier profile of the channel if the right conditions are chosen. Suppose a membrane is

[4]The influence of fixed charges on carrier-mediated transport was treated by Adrian (1969) and Roomans and Borst-Pauwels (1978).

clamped to an overall voltage which allows a cationic net current to flow into the cell. The outer bulk concentration of the permeant species is high and fixed charges at the outer membrane surface are titrated. If then the current decreases on removal of negative surface charges, transport is entrance-step limited and the channel occupancy is small. If the current increases (inverse titration curve), the transport is exit-step limited and the occupancy is large.

This occupancy rule applies to net cationic channel currents directed away from the fixed charge layer which is titrated. For net cationic current flowing oppositely, inverse titration curves are the sign of low channel occupancy (and vice versa), provided negative clamp voltages are used with a concentration gradient directed into the cell (c_i large). In contrast, if c_i is small and the concentration gradient is directed outward, c-control cannot dominate. In consequence the current titration curves are inverted at all occupancies.

Failure of the current to change does not prove the absence of fixed charges at the channel opening, because at certain overall clamp voltages a channel of intermediate occupancy may show little change of current when its surface charge density is varied. Only when over a large range of clamp voltages pH_0 has no effect on the channel current, i.e., when (at constant density of conducting channels) the whole current-voltage curve is invariant to pH_0, may we consider the possibility that the channel opening is free of titratable fixed charges.

The models that I used for double-layer properties and channel properties are intentionally simplistic. Details like discrete fixed charges with poor field overlap, cation binding, concentration polarization, saturation effects in the double layer as well as fixed charges at the protoplasmic opening of the channels were omitted as unnecessary for the point to be made. All numerical examples shown deal with symmetrical channels, but calculations made for asymmetrical barrier profiles yielded the same results: for the conditions specified, high occupancy causes the current titration curve to invert. High occupancy may be verified experimentally by varying the activity of the transported ion species in the bulk solution at constant ionic strength. However, should the macroscopic current saturate, one still has to exclude that the area density of conducting channels varies with ion concentration or bulk pH, as it has been shown to do in the apical membrane of frog skin epithelium (Van Driessche and Lindemann, 1979; Li and Lindemann, 1980).

"Inverse" titration curves can be based on a variety of mechanisms. Unintended pH changes at a fixed charge layer on the opposite membrane surface, poor channel selectivity which allows for proton currents at low pH, and pH-controlled conformational changes of the channel protein are examples. The purpose of this paper is merely to direct attention to another, equally basic, mechanism. The literature contains some examples of peaked or inverted titration curves. One well-known case is the anion exchange channel of erythrocytes. Schnell (1977) advanced a 1B2S-model with positive surface fixed charges and saturable anion adsorbtion sites at both ends of the channel to account for the peaked titration curve. In his model, too, the inverted branch of the curve, i.e., the decrease of anion transport with decreasing pH, was essentially due to high channel occupancy. Other examples for inverted titration curves were provided by studies of chloride transport in skeletal muscle and K transport in heart muscle and nerve. Hutter and Warner (1967) first discussed the inverted pH dependence of Cl conductance in terms of competition of protons and Ca ions for negative fixed charges. At presumably constant cellular pH high external pH might cause surface-charge reversal by increased Ca binding. This model was discarded because the titration curve showed a poor Ca dependence. The authors advanced an alternative explanation (see also Woodbury and Miles, 1973) which suggests a Cl channel containing an imidazole group. When protonated this group binds Cl ions more strongly, thus increasing Cl occupancy and decreasing Cl conductance. This model no longer specifies fixed charges at the external channel opening.

In the Purkinje fiber of heart muscle, the outward pacemaker K current (I_{K2}) at constant activation was found to decrease with external pH (Brown and Noble, 1978). This may point to a V-controlled titration curve which should be expected for K outward current. In these experiments a change of cellular pH may also be involved (see Van Bogaert et al. 1978), particularly because the activation curve of I_{K2} shifts inversely with external pH. K transport at the node of Ranvier was studied at low K gradients by Mozhayeva and Naumov (1972). Their data indicate V-controlled current titration curves at voltages near the reversal potential but outside of the voltage range where gating occurs. In contrast, Ohki (1978) found that in squid axons of more normal ionic gradients and fully activated channels, an increase of the external Ca concentration lowered the Na conductance. This result is compatible with c control and, therefore, with entrance-rate limited translocation and low occupancy. The decrease of conductance, however, was somewhat smaller than expected from a diffuse double-layer model. Na transport through the apical membrane of toad urinary bladder has a peaked titration curve (Leaf et al. 1964), which was tentatively explained by a carrier-mediated Na-proton cotransport. A similar titration curve was found for apical Na transport in the epidermis of *Rana ridibunda* (e.g., Zeiske and Lindemann, 1975).

I should like to thank Dr. H.-H. Kohler for a discussion (at the Titisee-conference in 1980) from which this study arose and Dr. B. Neumcke for valuable comments on the manuscript. The computer programs written for the numerical work (Fortran) will be made available to interested readers on request.

This work was supported by the Deutsche Forschungsgemeinschaft through the Sonderforschungsbereich 38, project C1.

Received for publication 15 September 1981 and in revised form 2 February 1982.

REFERENCES

Adrian, R. H. 1969. Rectification in muscle membrane. *Prog. Biophys. Mol. Biol.* 19:340–369.

Brown, R. H., and D. Noble. 1978. Displacement of activation thresholds in cardiac muscle by protons and calcium ions. *J. Physiol. (Lond.).* 282:333–343.

Drouin, H., and B. Neumcke. 1974. Specific and unspecific charges at the sodium channels of the nerve membrane. *Pflügers Arch. Eur. J. Physiol.* 351:207–229.

Eyring, H., R. Lumry, and J. W. Woodbury. 1949. Some applications of modern rate theory to physiological systems. *Recent Chem. Prog.* 10:100–114.

Frankenhaeuser, B. 1960. Sodium permeability in toad nerve and in squid nerve. *J. Physiol. (Lond.).* 152:159–166.

Goldman, D. E. 1943. Potential, impedance and rectification in membranes. *J. Gen. Physiol.* 27:37–60.

Heckmann, K., B. Lindemann, and J. Schnakenberg. 1972. Current-voltage curves of porous membranes in the presence of pore-blocking ions. I. Narrow pores containing no more than one moving ion. *Biophys. J.* 12:683–702.

Hodgkin, A. L., and B. Katz. 1949. The effect of sodium ions on the electrical activity of the giant axon of the squid. *J. Physiol. (Lond.).* 108:37–77.

Hutter, O. F., and A. E. Warner. 1967. The pH sensitivity of the chloride conductance of frog skeletal muscle. *J. Physiol. (Lond.).* 189:403–427.

Läuger, P. 1976. Diffusion-limited ion flow through pores. *Biochim. Biophys. Acta.* 455:493–509.

Leaf, A., A. Keller, and E. F. Dempsey. 1964. Stimulation of sodium transport in toad bladder by acidification of the mucosal medium. *Am. J. Physiol.* 207:547–552.

Li, J. H. -Y., and B. Lindemann. 1980. pH-dependence of apical Na-transport in frog skin. *Adv. Physiol. Sic.* 3:151–155.

Lindemann, B. 1968. Experimentelle und theoretische Untersuchungen des Na- und Wassertransportes durch das Epithel der Froschhaut. Thesis, Medizinische Fakultät. Universität des Saarlandes, Homburg/Saar 74–80..

McLaughlin, S. G. A., G. Szabo and G. Eisenman. 1971. Divalent ions and the surface potential of charged phospholipid membranes. *J. Gen. Physiol.* 58:667–687.

Mozhayeva, G. N., and A. P. Naumov. 1972. Effect of the surface charge on the steady state potassium conductivity of the membrane of a node of Ranvier. I. Change in pH of external solution. *Biofizika* 17:412–420.

Neumcke, B. 1976. Surface charges on nerve membranes and artificial lipid bilayers. *J. Electrochem. Soc.* 123:1331–1334.

Ohki, S. 1978. Ionic conductance and surface potential of axon membranes. *Bioelelctrochem. Bioenerg.* 5:204–214.

Parlin, B., and H. Eyring. 1954. Membrane permeability and electrical potential. *In* Ion transport across membranes. H. T. Clarke editor. Academic Press, Inc. New York. 103–118.

Roomans, G. M., and G. W. F. H. Borst-Pauwels. 1978. Cotransport of anions and neutral solutes with cations across charged biological membranes. Effects of surface potential in uptake kinetics. *J. Theoret. Biol.* 73:453–468.

Schnell, K. F. 1977. Anion transport across the red blood cell membrane mediated by dielectric pores. *J. Membr. Biol.* 37:99–136.

Van Driessche, W., and B. Lindemann. 1979. Concentration-dependence of currents through single sodium-selective pores in frog skin. *Nature (Lond.)* 282:519–520.

Van Bogaert, P. -P., J. S. Vereecke, and E. E. Carmeliet. 1978. The effect of raised pH on pacemaker activity and ionic currents in cardiac Purkinje fibers. *Pflügers Arch. Eur. J. Physiol.* 375:45–52.

Woodbury, J. W., and P. R. Miles. 1973. Anion conductance of frog muscle membranes: two kinds of pH dependence. *J. Gen. Physiol.* 62:324–353.

Woodbury, J. W., S. H. White, M. C. Mackey, W. L. Hardy, and D. B. Chang. 1970. Bioelectrochemistry. *In* Electrochemistry. H. Eyring, W. Jost, and D. Henderson, editors. Academic Press, Inc. New York. Chap. 9.

Zeiske, W., and B. Lindemann. 1975. Blockage of Na-channels in frog skin by titration with protons and by chemical modification of COO^--groups. *Pflügers Arch. Eur. J. Physiol.* 355:R72.